



This is a repository copy of *Computational studies on the reactions of thiols, sulfides and disulfides with hydroperoxides. Relevance for jet fuel autoxidation.*

White Rose Research Online URL for this paper:

<https://eprints.whiterose.ac.uk/220574/>

Version: Accepted Version

---

**Article:**

Parks, C.M. [orcid.org/0000-0001-8016-474X](https://orcid.org/0000-0001-8016-474X), Meijer, A.J.H.M. [orcid.org/0000-0003-4803-3488](https://orcid.org/0000-0003-4803-3488), Blakey, S.G. et al. (2 more authors) (2022) Computational studies on the reactions of thiols, sulfides and disulfides with hydroperoxides. Relevance for jet fuel autoxidation. Fuel, 316. 123326. ISSN 0016-2361

<https://doi.org/10.1016/j.fuel.2022.123326>

---

Article available under the terms of the CC-BY-NC-ND licence (<https://creativecommons.org/licenses/by-nc-nd/4.0/>).

**Reuse**

This article is distributed under the terms of the Creative Commons Attribution-NonCommercial-NoDerivs (CC BY-NC-ND) licence. This licence only allows you to download this work and share it with others as long as you credit the authors, but you can't change the article in any way or use it commercially. More information and the full terms of the licence here: <https://creativecommons.org/licenses/>

**Takedown**

If you consider content in White Rose Research Online to be in breach of UK law, please notify us by emailing [eprints@whiterose.ac.uk](mailto:eprints@whiterose.ac.uk) including the URL of the record and the reason for the withdrawal request.



[eprints@whiterose.ac.uk](mailto:eprints@whiterose.ac.uk)  
<https://eprints.whiterose.ac.uk/>

1 Computational studies on the Reactions of Thiols,  
2 Sulfides and Disulfides with Hydroperoxides.  
3 Relevance for Jet Fuel Autoxidation.

4  
5 *Christopher M. Parks\**<sup>a</sup>, *Anthony J.H.M. Meijer*<sup>b</sup>, *Simon G. Blakey*,<sup>c</sup> *Ehsan Alborzi*<sup>a</sup>

6 *Mohamed Pourkashanian*<sup>a</sup>

7  
8 <sup>a</sup> *Department of Mechanical Engineering, The University of Sheffield, Sheffield S3 7RD, UK*

9 <sup>b</sup> *Department of Chemistry, The University of Sheffield, Sheffield, S3 7HF*

10 <sup>c</sup> *Department of Mechanical Engineering, The University of Birmingham, Birmingham B15*

11 *2TT, U.K.*

12  
13 *Email:* [c.m.parks@sheffield.ac.uk](mailto:c.m.parks@sheffield.ac.uk), [e.alborzi@sheffield.ac.uk](mailto:e.alborzi@sheffield.ac.uk), [S.G.Blakey@bham.ac.uk](mailto:S.G.Blakey@bham.ac.uk),

14 [a.meijer@sheffield.ac.uk](mailto:a.meijer@sheffield.ac.uk)

15  
16 **Abstract**

17  
18 Density Functional Theory calculations (DFT) are reported on the reactions of hydroperoxides  
19 with different classes of sulfur: thiols (RSH), sulfides (RSR) and disulfides (RSSR), all of  
20 which are important trace species in the auto-oxidation of jet fuel. It is shown that thiols can  
21 react under auto-oxidation conditions with hydroperoxides to form sulfonic acids and alcohols.  
22 In contrast, it is shown that disulfide species are more likely to form thiyl radicals, which are

23 less likely to be important for the direct autoxidation of fuels due to prohibitive reaction  
24 barriers. The reaction mechanisms reported here for sulfur oxidation and the associated  
25 calculated thermodynamic data can be used to extend the applicability of current chemical  
26 kinetic models for fuel autoxidation, which are currently treated as a single elementary reaction  
27 despite the range of sulfur species found in fuels.

28

29 **Keywords:** DFT, Fuel autoxidation, Sulfur oxidation, Reaction Mechanisms.

30

## 31 **Introduction**

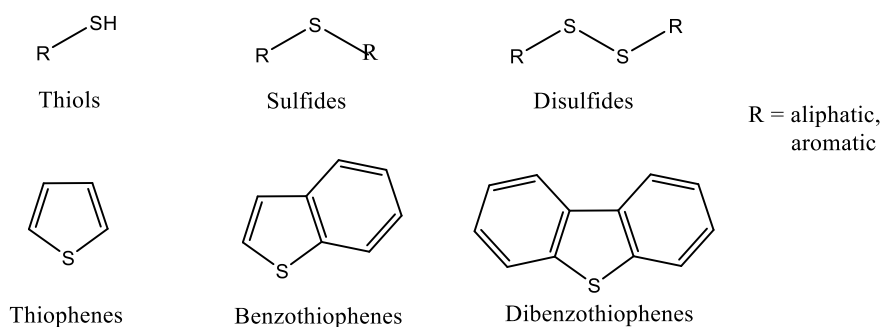
32

33 Jet fuel is primarily comprised of a blend of aliphatic and aromatic hydrocarbons as well as  
34 low levels of hydroperoxides and trace heteroatomic species (the latter generally in ppm  
35 quantities). The hydrocarbons afford the fuel its bulk properties such as viscosity, density and  
36 volatility which are not only important when it is used as a propellant, but also when exploited  
37 as a coolant as happens in modern aircraft. In the latter use, at temperatures of approximately  
38 140 °C a process called autoxidation is initiated. Here a series of chemical reactions can occur  
39 that can lead to both bulk and surface deposits. Experimentally, it has been shown that many  
40 species can have an effect on this process including sulfur compounds<sup>1-3</sup>, polar species<sup>4-9</sup>,  
41 dissolved metals<sup>10, 11</sup> and hydroperoxides.<sup>12, 13</sup> A number of studies have reported on the  
42 thermal stability of jet fuel, with a focus on the oxidative mechanisms involved therein.<sup>14-21</sup>

43

44 In the current paper, we focus on the reactions between sulfur species and hydroperoxides. A  
45 number of different classes of sulfur compounds can be present in jet fuels as shown in **Figure**

46 1. They include thiols (RSH), sulfides (RSR), disulfides (RSSR), thiophenes,  
47 benzothiophenes, dibenzothiophenes and substituted variants thereof. Oxidized variants of  
48 these such as sulfoxides and sulfonic acids can either be present initially or formed through  
49 reactions with oxygen and hydroperoxides. Multiple studies have focused on classifying the  
50 types of sulfur species present in aviation fuel. In these studies, several analytical techniques  
51 were employed to separate sulfur species from aviation fuels and gasolines. They were  
52 subsequently classified as reactive and non-reactive sulfurs and further subcategorized as  
53 thiols, sulfides, disulfides, thiophenes, benzothiophenes and substituted benzothiophenes.<sup>22-24</sup>  
54 .



55

56 **Figure 1:** General structures of common sulfur species found in jet fuel.

57

58 The exact nature of the role of sulfur in jet fuel is still being debated in the literature. Indeed,  
59 there are a number of reviews on the subject with contrasting views.<sup>8, 25-29</sup> Irrespective of this  
60 debate, it has been accepted that sulfur species react with hydroperoxides in the fuel as in  
61 **Figure 2.** This sulfur-hydroperoxide reaction proceeds *via* a non-radical mechanism to form  
62 oxidized sulfur compounds and alcohols.<sup>30</sup> This process results in a reduction in the  
63 hydroperoxide concentration, which could in turn retard the rate of autoxidation of the fuel.

64



65

66 **Figure 2:** Reaction of hydroperoxides and sulfides to form alcohols and sulfones. (R =  
 67 aliphatic, aromatic)

68

69 A number of literature studies have reported on the effects of sulfur species on jet fuel  
 70 autoxidation. In 1976, Taylor showed that thiophenes and disulfide species contribute  
 71 significantly to deposition.<sup>8</sup> Moreover, dibenzothiophenes were found to have little effect on  
 72 deposition. These observations were further corroborated by Mushrush et al. who showed that  
 73 thiophenes and thiophenols have a destabilizing effect on jet fuel.<sup>29</sup> Further work by  
 74 Offenhauer and Hiley showed that both sulfonic acids and thiophenols increased both  
 75 deposition and gum formation whereas diaryl sulfides have little effect.<sup>31, 32</sup> The proposed dual  
 76 roles that sulfur compounds can play was reported by both Denison et al. and Thompson et  
 77 al..<sup>33, 34</sup> They observed that disulfides decreased the thermal stability of the fuel. In contrast,  
 78 aliphatic sulfides had a small stabilizing effect. In a series of experimental studies, Daniel and  
 79 Henemen doped jet fuel with different sulfur species at a range of concentrations.<sup>35</sup> Thiols and  
 80 thiophenes decreased the thermal stability whilst disulfides and sulfides increased the thermal  
 81 stability. The largest amount of deposits were observed by Rawson et al. for model fuels doped  
 82 with benzylosulfonic acid, diphenyl disulfide and elemental sulfur.<sup>36</sup> The contrasting results in  
 83 many of these studies highlight the complex nature of the underlying mechanisms.

84

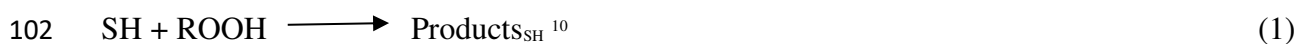
85 Despite the importance of these trace sulfur species in jet fuel, there has only been a limited  
 86 number of computational studies into the energetics of the reactions involving these species.  
 87 Bach and co-workers investigated the activation energy for the reaction of Me<sub>2</sub>S with

88 methylperoxide (MeOOH) and tert-butyl peroxide (<sup>t</sup>BuOOH), which were calculated to be 32.4  
89 and 32.2 kcal mol<sup>-1</sup> respectively.<sup>37</sup> In these calculations it was shown for the first time that the  
90 transition state is concerted. In particular, the hydroxyl oxygen atom in the hydroperoxide is  
91 transferred to the sulfur as the hydrogen moves to form the alcohol. More recently, Zabarnick  
92 et al. modelled the reactions of Et<sub>2</sub>S and EtSSEt with <sup>n</sup>BuOOH.<sup>30</sup> The activation energies for  
93 these reactions were 26.1 and 28.7 kcal mol<sup>-1</sup>.

94

95 The lack of detailed investigations into the reactions of sulfur compounds and hydroperoxides  
96 prompted our investigation. Current chemical kinetic models, which aim to predict the rate of  
97 fuel autoxidation describe sulfur chemistry using one elementary reaction (**equation 1**).<sup>10</sup>  
98 Given the wide range of sulfur species that could be present in jet fuels, it is likely that the  
99 applicability of such kinetic models could be improved by a more thorough understanding of the  
100 individual reactions each sulfur species could undergo.

101



103

104 In this paper, we report on a series of DFT calculations on a large range of sulfur compounds,  
105 which are each in turn reacting with multiple hydroperoxides. Further reactions beyond the  
106 initial oxidation are considered. The different routes to the formation of sulfones and sulfonic  
107 acids are also probed. The propensity of disulfide species to undergo fission reactions and  
108 form thiyl radicals are also investigated as are the potential implications of the formation of  
109 such species. In its entirety, our work provides an extensive thermochemical library for sulfur–  
110 peroxide reactions to further improve current kinetic models for aviation fuel degradation.

111

112

## 113 2 Experimental and computational Details

114

115 An analysis of a sample of Jet A-1 fuel was conducted in order to determine which sulfur  
116 species were the most appropriate to model. Jet A-1 fuel samples were analysed for sulfur  
117 content using an in-house method. This method identifies the sulfur species in middle  
118 distillates using an Agilent 7890N Gas chromatogram combined with a Zoex thermal  
119 modulation and chemiluminescence detector. Quantification of the types of sulfur species  
120 present was achieved through normalization against the total sulfur content of the fuel sample  
121 as determined by combustion followed by UV fluorescence analysis. This analytical method  
122 separates all the sulfur-containing compounds according to their boiling point and polarity.  
123 This afforded the ability to differentiate between benzothiophenes and dibenzothiophenes  
124 observed as two well-defined bands, which were well separated from the lower polarity  
125 thiophenes, mercaptans and sulfides.<sup>38-40</sup>

126

127 DFT calculations were performed using Gaussian 09 software<sup>41</sup>, version D.01, using Gaussian-  
128 supplied versions of BLAS and ATLAS.<sup>42, 43</sup> All calculations used the B3LYP functional.<sup>44-46</sup>  
129 The cc-pVTZ basis set was used for all elements.<sup>47</sup> Benchmarking studies show this setup to  
130 be acceptable.<sup>16, 19</sup> In all calculations solvent was accounted for by the polarizable continuum  
131 model (PCM) method using solvent parameters for dodecane as implemented in Gaussian.<sup>48, 49</sup>  
132 Calculations were carried out at 298.15 K. Geometry optimizations were confirmed to be local  
133 minima by the absence of imaginary frequencies in the vibrational spectra. Transition states  
134 were optimized using the QST3 method as implemented in Gaussian.<sup>50</sup> All transition states  
135 were confirmed both visually *via* the presence of one large imaginary frequency corresponding  
136 to the saddle point and *via* intrinsic reaction coordinate (IRC) scans. An ultrafine grid was  
137 employed for all calculations with no symmetry constraints. Radical species were calculated

138 as singlets with the HOMO and LUMO orbitals mixed (guess=mix option) in order to break  
139 the symmetry of the system. Free energies were calculated using the Grimme quasiharmonic  
140 entropy correction using the GoodVibes script.<sup>51</sup> Selected stationary points were improved with  
141 coupled cluster calculations (CCSD(T)) using MolPro.<sup>52</sup> Quoted values in the manuscript are  
142 subject to an error of  $\pm 2.5$  kcalmol<sup>-1</sup> based upon benchmarking studies.<sup>16, 19</sup>

143

144 Activation energies are calculated as the energy difference between the transition state and both  
145 reactants at infinite separation. Arrhenius pre-exponential factors were calculated according  
146 to **equation 2**.

147

$$148 \quad A = \frac{k_b T}{h} \exp\left(\frac{\Delta S}{R}\right) \quad (2)$$

149

## 150 **3 Results and Discussion**

### 151 **3.1 Sulfur selection**

152 **Table 1:** Results from the analysis of sulfur content in a Jet A-1 fuel sample

Sulfur species	Amount detected / %
Thiols, sulfides and disulfides	57
Dibenzothiophenes	26
Unknown	12
Dibenzothiophenes	2
Benzothiophenes	2
Substituted dibenzothiophenes	1

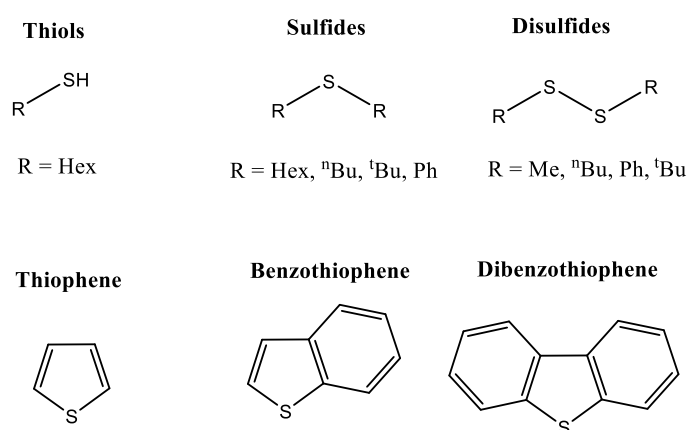
153

154 In order to guide our computational investigations, we initially conducted a speciation analysis  
155 of a JetA-1 fuel using GC x GC as described in the experimental section. The results of this  
156 analysis are shown in **Table 1**. By far, the most abundant sulfur species detected were thiols,  
157 disulfides and sulfides (57 %). These were followed by substituted benzothiophenes (26.0 %)



158 and dibenzothiophenes (12.0 %). A small quantity of non-substituted benzothiophenes were  
159 also detected. Based upon these observations, the species shown in **Figure 3** were selected for  
160 computational analysis. For thiols, sulfides and disulfides a mixture of aromatic and aliphatic  
161 R groups were selected. These were chosen to provide as wide a selection of structures as  
162 possible within the range of compounds detected in the jet fuel sample.

163



164

165 **Figure 3:** Structures of sulfur species selected for computational analysis

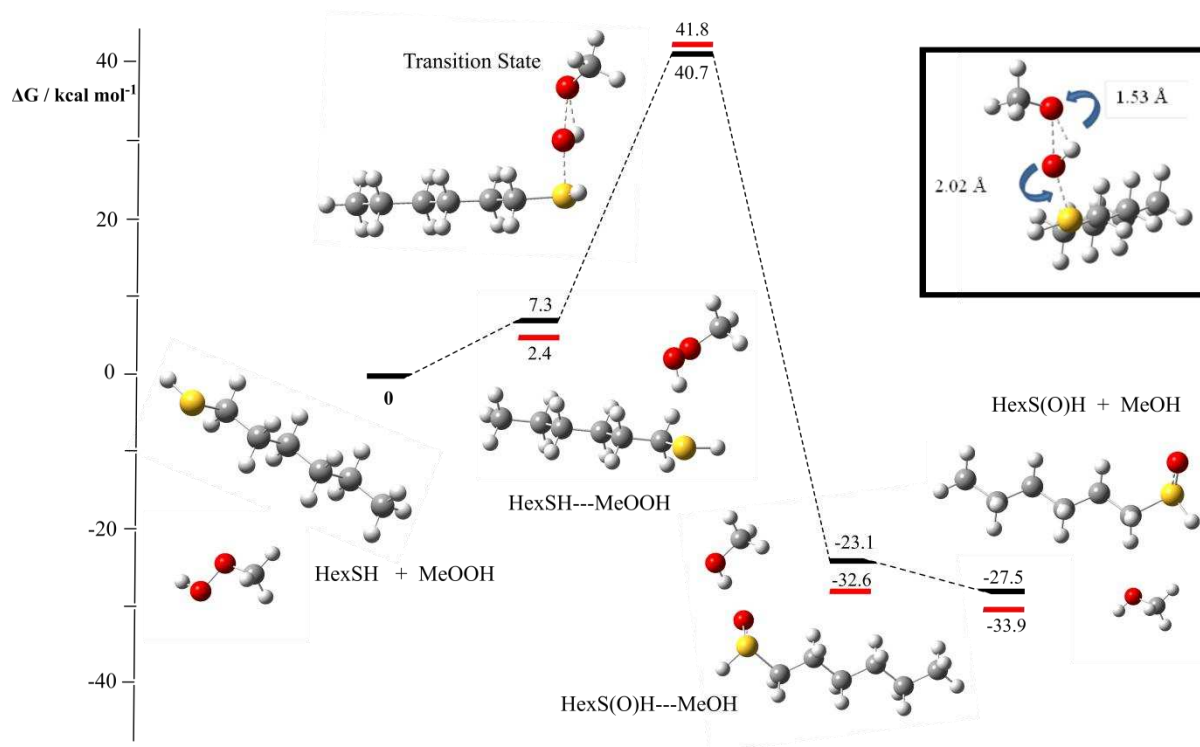
166

### 167 3.2 Reactions of thiols and sulfides with hydroperoxides

168

169 Our computational studies were initially focused on how the aforementioned sulfur species  
170 might affect autoxidation by investigating how they react with hydroperoxides. It has  
171 previously been reported that sulfur species react with hydroperoxides to form alcohols and  
172 oxidized sulfur species through a non-radical pathway.<sup>29</sup> Our initial studies focused on the  
173 reactions of thiols (general formula RSH). The energy profile for the reaction of hexane thiol  
174 and methyl hydroperoxide is shown in **Figure 4**.

175



176

177 **Figure 4:** Gibbs free energy profile for the reaction of hexane thiol and MeOOH. Inset:

178 Transition state structure. Results from CCSD(T) calculations shown in red.

179

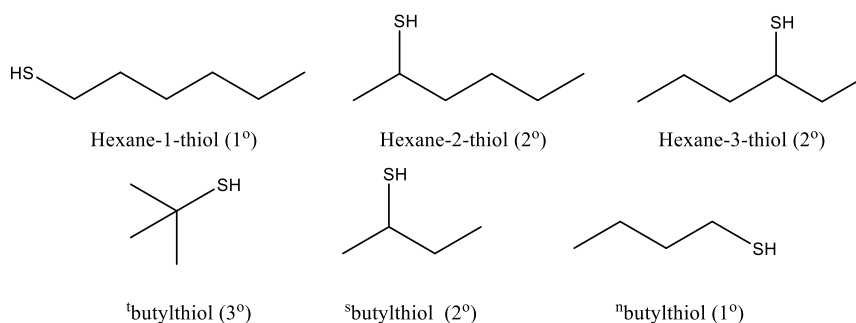
180 The pre-reaction complex, (HexSH---MeOOH in **Figure 4**) is defined as the structure where  
 181 the two reactants are in close proximity immediately prior to the reaction taking place. Here,  
 182 the pre-reaction complex is 7.3 kcal mol<sup>-1</sup> less stable than the separated reactants. The  
 183 transition state geometry is shown inset in **Figure 4**. The hydroxyl oxygen of the incoming  
 184 hydroperoxide is transferred to the sulfur atom of the thiol. Concurrently, the hydroxyl  
 185 hydrogen is transferred back to form an alcohol. The activation free energy for this reaction is  
 186 40.7 kcal mol<sup>-1</sup> and the reaction free energy is -27.5 kcal mol<sup>-1</sup>.

187

188 Next, we considered the effect of the chosen hydroperoxide on the activation energy. It is  
 189 computationally efficient to conduct these calculations using MeOOH as a model for the  
 190 hydroperoxides found in jet fuel. However, it is not a representative structure. Fuel  
 191 hydroperoxides will contain a much longer carbon chain or could be derived from branched

192 paraffinic species. Therefore, we investigated the reactions with different hydroperoxides to  
193 ascertain whether MeOOH was an appropriate model. To address this, we calculated the same  
194 energy profile as shown in **Figure 4**, replacing MeOOH with a range of linear alkyl peroxides  
195 (Carbon numbers 1 to 12) and two branched hydroperoxides – cumene hydroperoxide (CHP)  
196 and <sup>t</sup>BuOOH. The effect on the activation energy and reaction energy of increasing chain  
197 length is presented in **Figure S3** in the supporting information.

198  
199 As can be seen from **Figure S3**, the effect of increasing the hydroperoxide chain length on both  
200 the activation free energy and reaction free energy is small. In particular, activation free  
201 energies range from 40.7 - 42.4 kcal mol<sup>-1</sup>. Reaction free energies range from -33.6 to -34.3  
202 kcal mol<sup>-1</sup>. A reduction in the activation free energy to 39.95 kcal mol<sup>-1</sup> is noted when CHP is  
203 used as the model hydroperoxide. The corresponding value for <sup>t</sup>BuOOH is 41.5 kcal mol<sup>-1</sup>. In  
204 light of these results, further studies hereafter are carried out using both MeOOH, <sup>t</sup>BuOOH and  
205 CHP. MeOOH was chosen as it clearly is an acceptable model for the larger linear-chained  
206 hydroperoxides. Moreover, it can be modelled in a timely manner. CHP and <sup>t</sup>BuOOH were  
207 chosen as more realistic fuel peroxides for aromatic and branched hydroperoxides respectively.  
208 Data for the reactions of sulfur species and both <sup>t</sup>BuOOH and CHP can be found in the  
209 supporting information and is collated in **Table 3**.



210  
211 **Figure 5:** Primary (1°), secondary (2°) and tertiary (3°) thiol species selected for  
212 investigation

213

214 Consideration was also given as to how branching in the sulfur species affects the reactivity  
 215 with hydroperoxides. Several sulfur species were selected for investigation as shown in **Figure**  
 216 **5**, containing primary, secondary and tertiary thiols. In each case, the reaction with MeOOH  
 217 was modelled. The Gibbs free activation and reaction energies are collated in **Table 2**. As can  
 218 be seen, branching of the carbon chain has a minimal effect on both the Gibbs free activation  
 219 and reaction energies for the first oxidation reaction. This suggests that, at least for thiols  
 220 containing only carbon chains and no further functional groups, linear thiols can be investigated  
 221 as model complexes.

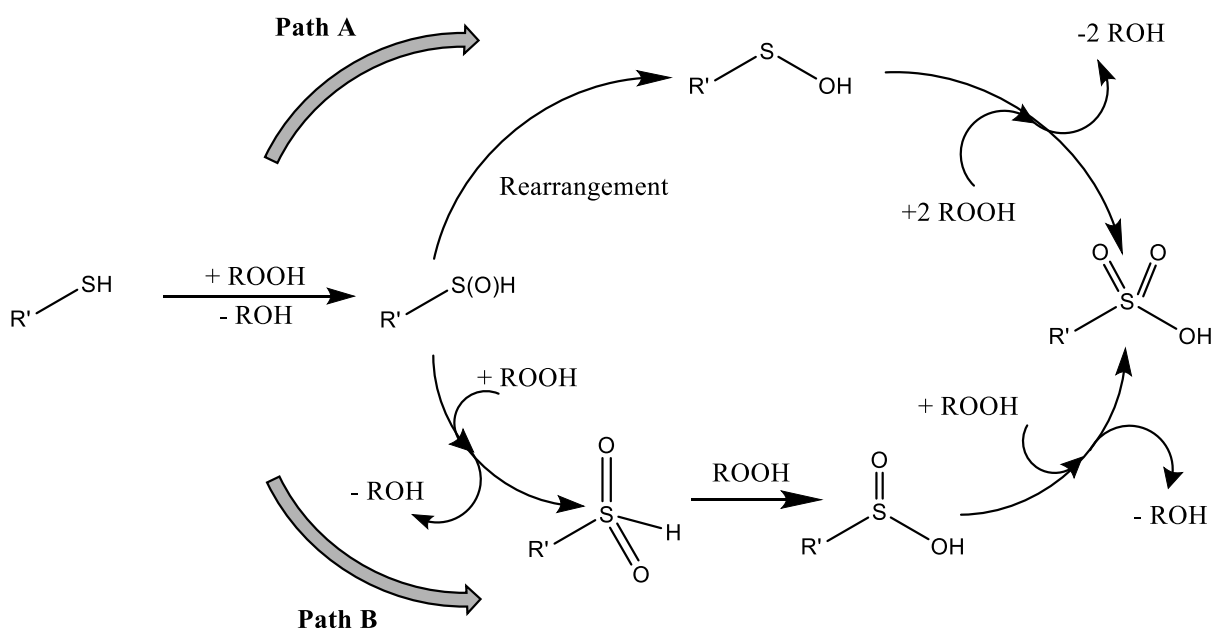
222

223 **Table 2:** Collated Gibbs free activation and reaction energies for the reaction of primary  
 224 (1°), secondary(2°) and tertiary thiols (3°) and MeOOH.

Sulfur species (type)	Gibbs free activation energy / kcal mol <sup>-1</sup>	Gibbs reaction energy
Hexane-1 thiol (1°)	41.8	-27.5
Hexane-2 thiol (2°)	40.9	-27.0
Hexane-3 thiol (2°)	42.6	-25.7
<sup>n</sup> butylthiol (1°)	41.8	-25.7
<sup>s</sup> butylthiol (2°)	40.8	-28.0
<sup>t</sup> butylthiol (3°)	40.4	-29.1

225

226



227

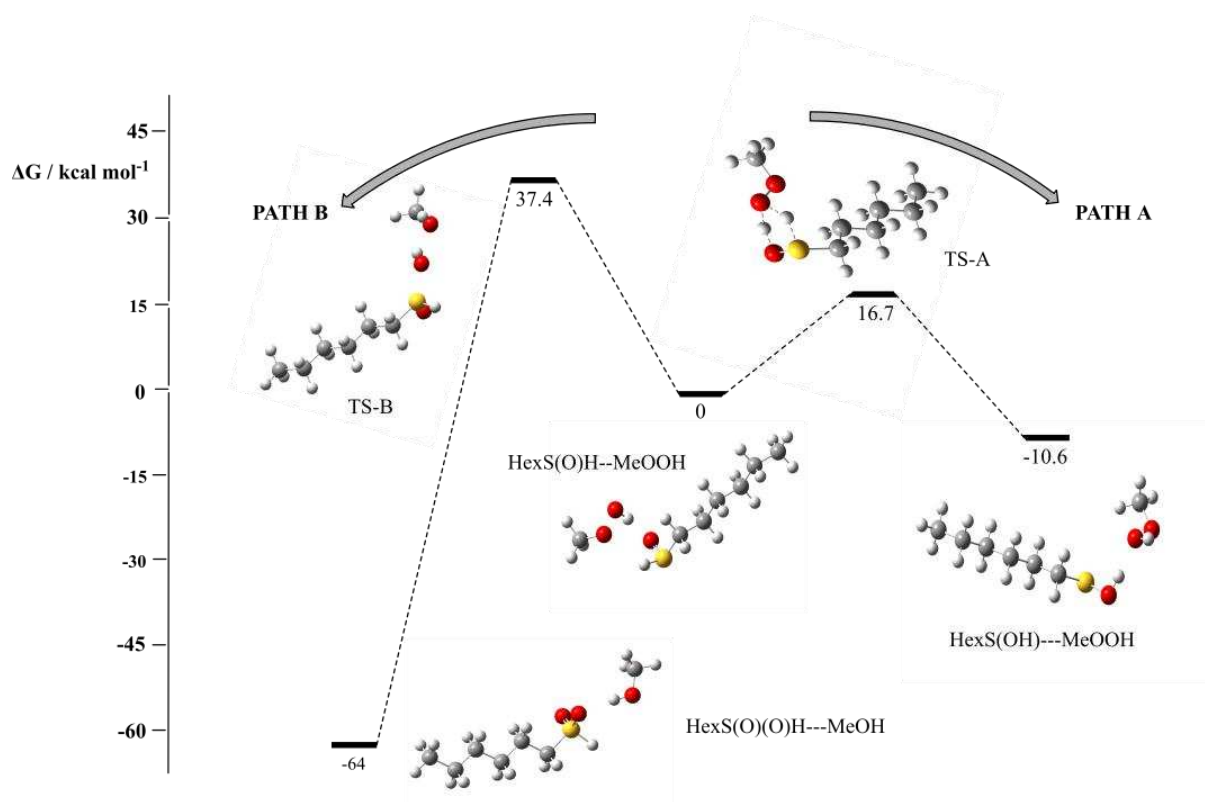
228 **Scheme 1:** Two potential mechanistic pathways leading to formation of  $RS(O)(O)OH$ .

229

230 Having considered the effect of both branching in the sulfur species and how the hydroperoxide  
 231 chain length affects the reactivity, we turned our attention to the subsequent reactions that the  
 232 oxidized thiol can undergo. The reaction of hexanethiol and  $MeOOH$  from **Figure 4** initially  
 233 forms an oxidized sulfur species ( $RS(O)H$ ) and an alcohol. Through successive further  
 234 oxidations it can form a sulfonic acid ( $RS(O)(O)OH$ ). This can occur through two distinct  
 235 routes as illustrated in **Scheme 1**. The oxidized sulfur species can first rearrange to form a  
 236 sulfenic acid ( $RS(OH)_2$ ) which can subsequently undergo two further oxidation reactions with  
 237 hydroperoxides to form the sulfonic acid (**path A** in **Scheme 1**). Alternatively, two further  
 238 oxidation reactions can occur either side of a rearrangement to form  $RS(O)(O)OH$  (**path B** in  
 239 **Scheme 1**). The energy profile illustrating the two divergent pathways starting from  $RS(O)H$ -  
 240  $-ROOH$  is presented in **Figure 6**.

241

242



243

244 **Figure 6:** Gibbs free energy profile illustrating the two reactions that oxidized hexanethiol  
 245 can undergo with MeOOH.

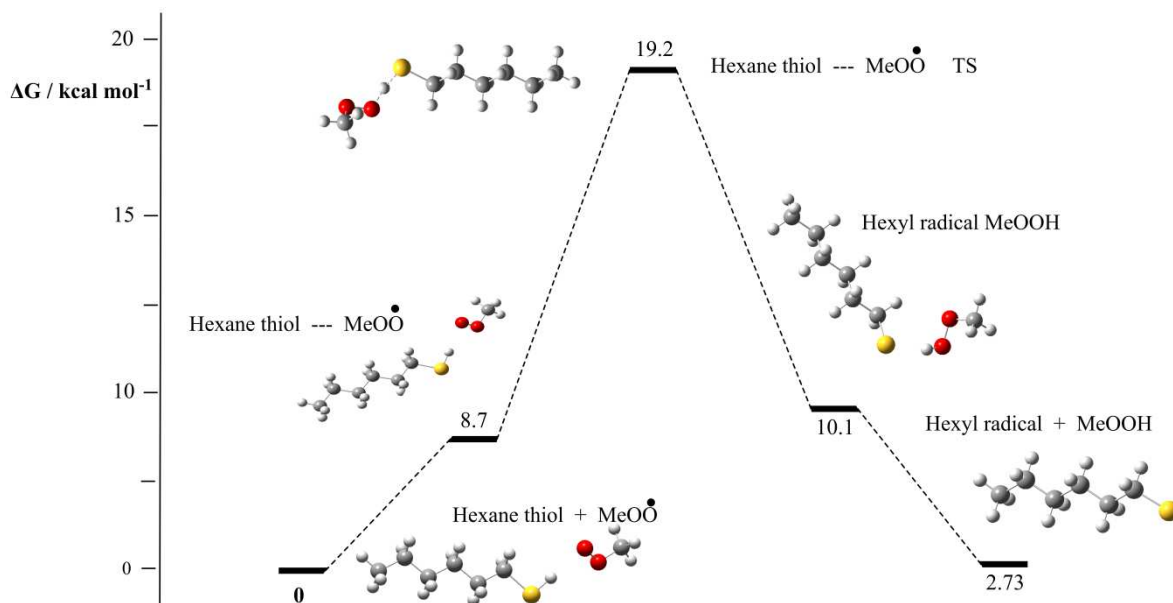
246

247 The activation free energy for the oxidation of HexS(O)H to HexS(O)(O)H is 37.4 kcal mol<sup>-1</sup>.  
 248 (path B in Figure 6) This is significantly larger than the activation free energy for re-  
 249 arrangement to form a sulfenic acid, HexS(OH) (16.7 kcal mol<sup>-1</sup>). Thus, the calculation  
 250 suggests that re-arrangement occurs prior to further oxidation. Activation free energies for  
 251 subsequent oxidations starting from a sulfenic acid are 23.1 kcal mol<sup>-1</sup> and 33.1 kcal mol<sup>-1</sup> for  
 252 the transformation of HexSOH to HexS(O)(O)H and HexS(O)(O)H to HexS(O)(O)OH  
 253 respectively. This data is provided in the supporting information.

254

255 We note that in a recent publication, we showed that the concentration of hydroperoxides  
 256 decreases significantly with each successive oxidation.<sup>53,54</sup> As a consequence, each successive  
 257 oxidized sulfur species will be present in a much lower concentration than the initial non-

258 oxidized sulfur compound. Thus, it is likely that only the initial oxidation reaction will be  
259 important in jet fuel given that further oxidation reactions will occur with a low frequency. Of  
260 course, the significance of each successive reaction may increase for fuels containing a higher  
261 concentration of hydroperoxides.



262

263 **Figure 7:** Gibbs free energy profile for the reaction of hexanethiol and MeOO•.

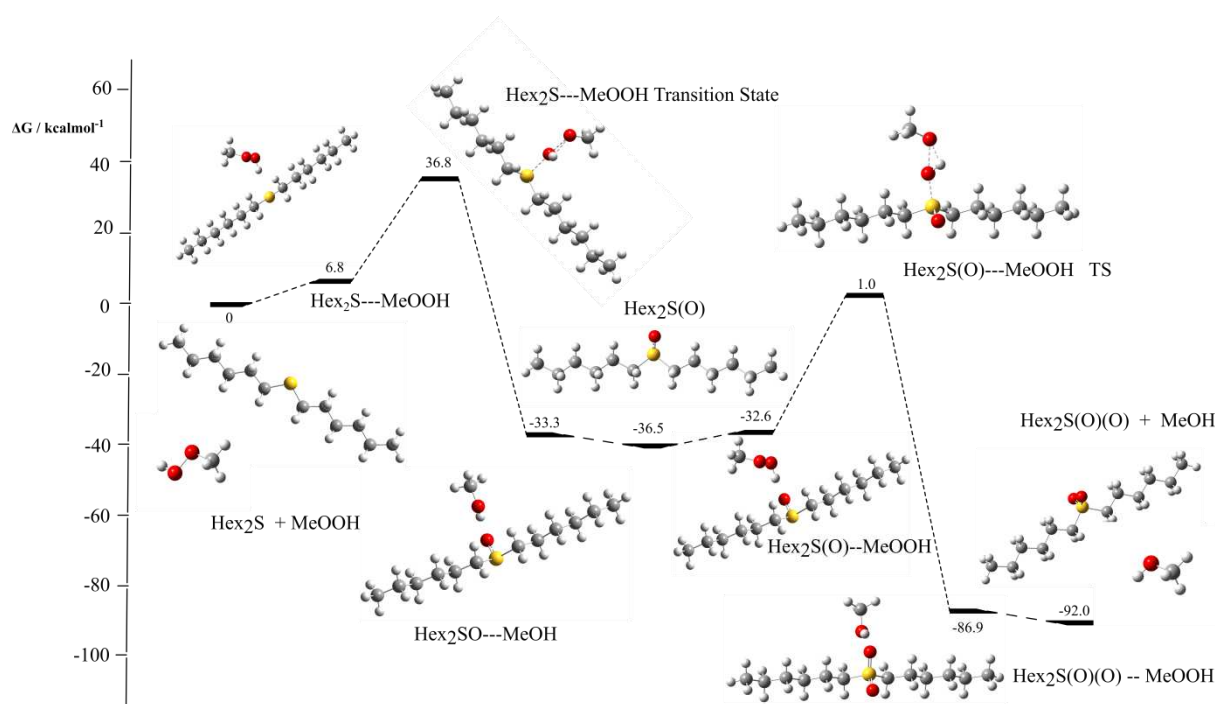
264

265 Our final consideration regarding thiol reactivity concerned the possibility of thiols reacting  
266 with peroxy radicals. Given that sulfur species have been shown to produce widely varying  
267 effects on jet fuel autoxidation and deposition, it is likely that they react with more than just  
268 hydroperoxides. Consequently, we investigated the reaction of hexane thiol and MeOO•. The  
269 Gibbs free energy profile is shown in **Figure 7**. This reaction has a free activation energy of  
270  $19.2 \text{ kcal mol}^{-1}$  and the overall reaction is only marginally uphill. This data suggests that thiols  
271 can react with peroxy radicals and generate hydroperoxides and thiyl radicals. Further  
272 investigations of the reactions that thiyl radicals can undergo will be detailed in **section 3.4**.

273

274 Sulfides were the next class of compounds to be investigated. Sulfides have the general formula  
 275 RSR. They can undergo similar reactions with hydroperoxides as observed for thiols.  
 276 However, in this case, there is a maximum of two oxidation steps. Moreover, sulfenic acid  
 277 cannot be formed because there is no terminal –SH bond. The free energy profile for the  
 278 reaction of hexyl sulfide and MeOOH is shown in **Figure 8**.

279



280

281 **Figure 8:** Gibbs free energy profile for the reaction of hexylsulfide and MeOOH.

282

283 The activation free energy for the oxidation of Hex<sub>2</sub>S to Hex<sub>2</sub>S(O) is 36.8 kcal mol<sup>-1</sup>, which is  
 284 similar to the activation free energy for the oxidation of hexane thiol. The second oxidation  
 285 reaction has an activation free energy of 37.5 kcal mol<sup>-1</sup>. Both of these reactions are permissible  
 286 given the standard conditions experienced during autoxidation (temperatures of between 140  
 287 and 300 °C). Corresponding activation energies for the reaction of CHP and Hex-S-Hex are  
 288 36.7 kcal mol<sup>-1</sup> and 37.4 kcal mol<sup>-1</sup> for the conversion of Hex<sub>2</sub>S to Hex<sub>2</sub>S(O) and Hex<sub>2</sub>S(O) to  
 289 Hex<sub>2</sub>S(O)(O) respectively.



290 **Table 3:** Collated Gibbs free activation energies for the first and second oxidation reactions  
291 between three sulfides and MeOOH.

Sulfur species	Gibbs free activation energy / kcal mol <sup>-1</sup>	
	First oxidation	Second oxidation
phenylsulfide	39.3	39.3
<sup>n</sup> butylsulfide	36.6	37.4
<sup>t</sup> butylsulfide	35.3	35.0

292  
293 **Table 3** contains calculated Gibbs free activation energies for the reaction of three further  
294 sulfides with MeOOH. The chosen sulfides contained phenyl, <sup>n</sup>butyl and <sup>t</sup>butyl substituents.  
295 As can be seen in **Table 3**, the first and second oxidation reactions of <sup>n</sup>butylsulfide and MeOOH  
296 are very similar to those calculated in **Figure 8**. As the only change between <sup>n</sup>butylsulfide and  
297 hexylsulfide is a reduction in the carbon chain length, this result is to be expected. The first  
298 and second oxidation reactions of phenylsulfide and MeOOH are higher than those reported  
299 for hexylsulfide

300

### 301 **3.3 Reactions of thiophenes, benzothiophenes and dibenzothiophenes**

302

303 The speciation analysis that we carried out on jet fuel indicated that substituted benzo- and  
304 dibenzothiophenes were the most observed species after thiols, sulfides and disulphides.  
305 However, the analysis did not provide information as to the exact nature and location of the  
306 substitutions. Due to this, we next investigated non-substituted analogues (ie, thiophene,  
307 benzothiophene and dibenzothiophenes) as models for these species.

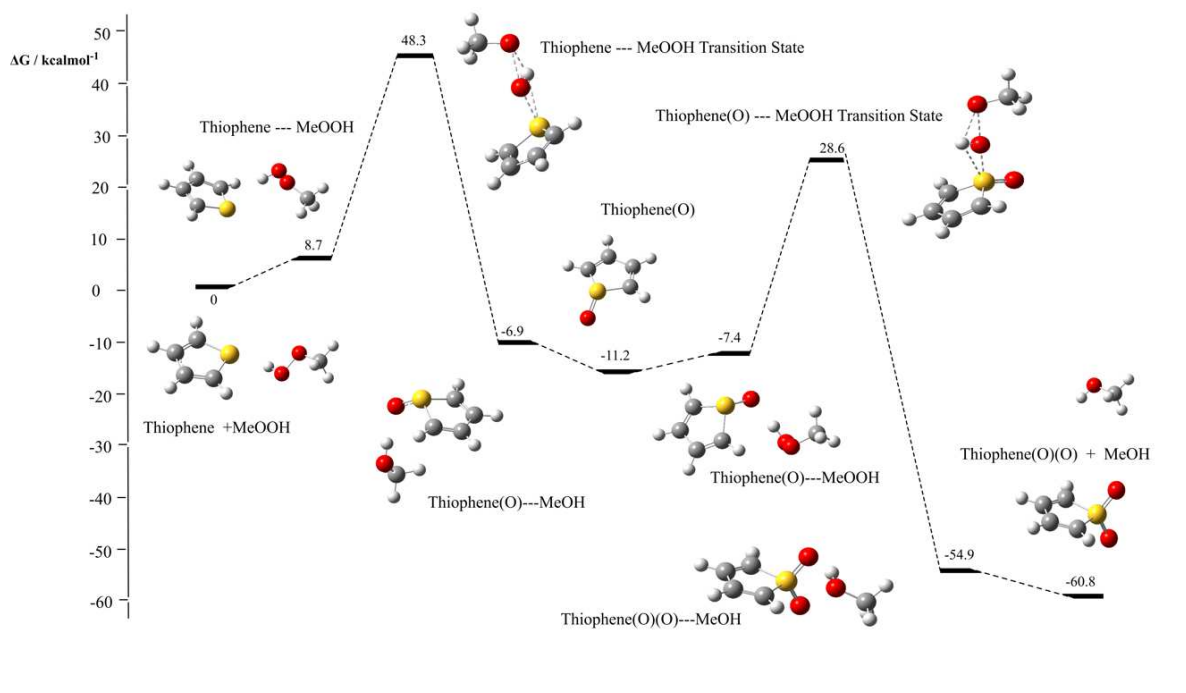
308

309 **Figure 9** shows the calculated energy profile for the reaction of thiophene and MeOOH.

310 Thiophene can undergo two successive oxidations with hydroperoxides as was the case for

311 sulfides (RSR). The activation free energy for the oxidation of thiophene to thiophene(O) is  
312 48.3 kcal mol<sup>-1</sup>. The subsequent oxidation reaction to thiophene(O)(O) has an activation free  
313 energy of 39.7 kcal mol<sup>-1</sup>.

314



315

316 **Figure 9:** Gibbs free energy profile for the reaction of thiophene and MeOOH.

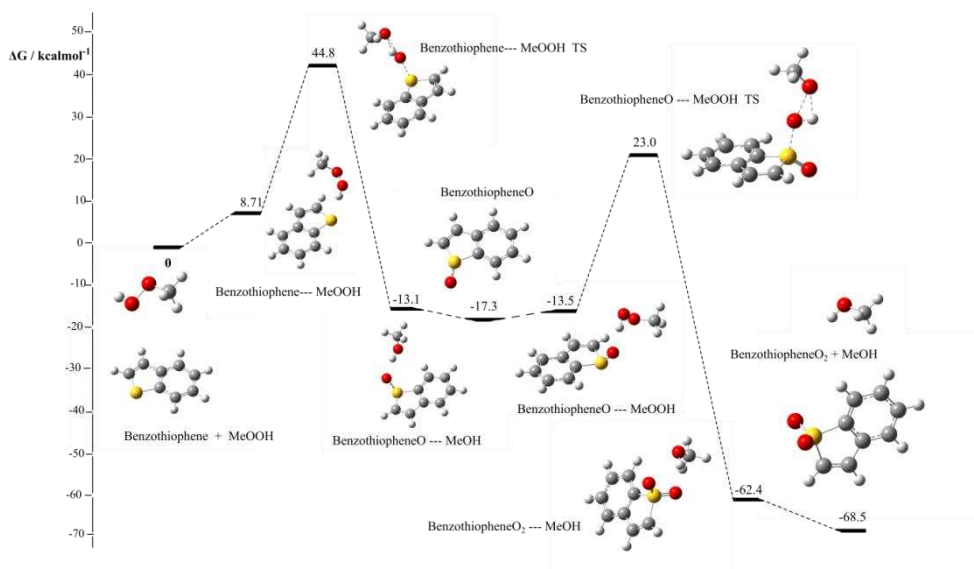
317

318 As can be seen in **Figures 10** and **11**, similar activation free energies were calculated for the  
319 reactions of both benzothiophene and dibenzothiophene with MeOOH. The calculated  
320 activation free energies for the first and second oxidation of benzothiophene are 44.8 and 40.3  
321 kcal mol<sup>-1</sup>. The first and second oxidation reactions of dibenzothiophenes have activation free  
322 energies of 43.2 and 40.7 kcal mol<sup>-1</sup>.

323

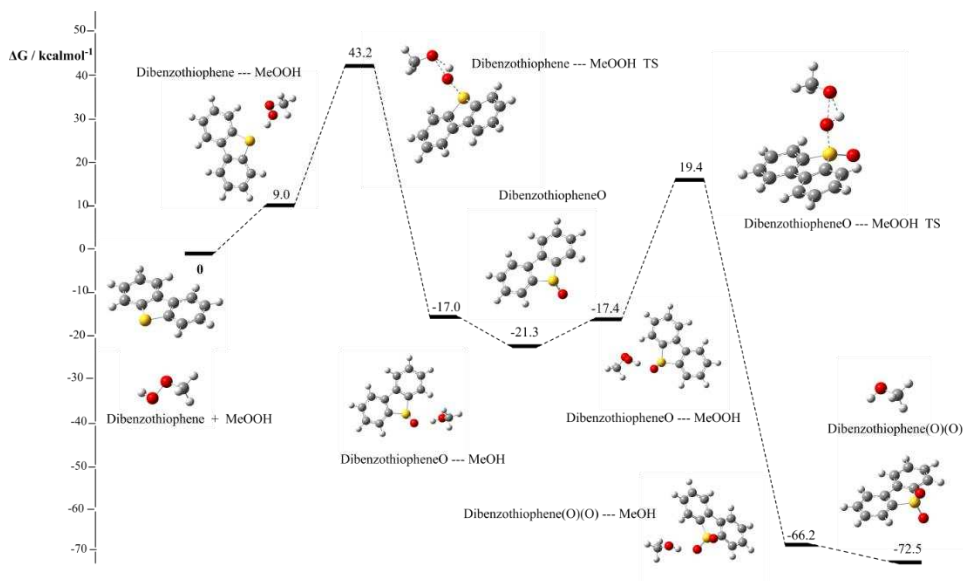
324 The calculated activation free energies for the first reaction between hydroperoxides and each  
325 of thiophene, benzothiophene and dibenzothiophene are higher than those calculated for  
326 hexylsulfide. This is attributed to the loss in aromaticity during the oxidation.<sup>55</sup>

327



328

329 **Figure 10:** Gibbs free energy profile for the reaction of benzothiophene and MeOOH.



330

331 **Figure 11:** Gibbs free energy profile for the reaction of dibenzothiophene and MeOOH.

332

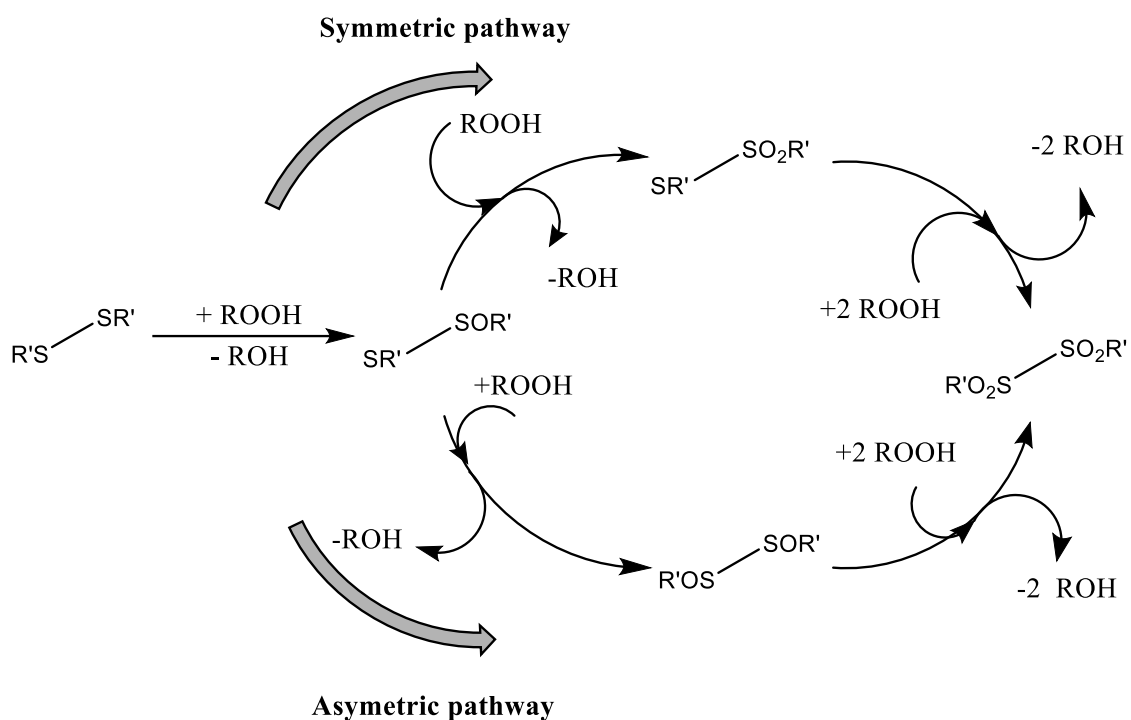
333

334

335

336

337



339

340 **Scheme 2:** Two potential mechanistic pathways leading to formation of  $\text{RSO}_2\text{SO}_2\text{R}$ .

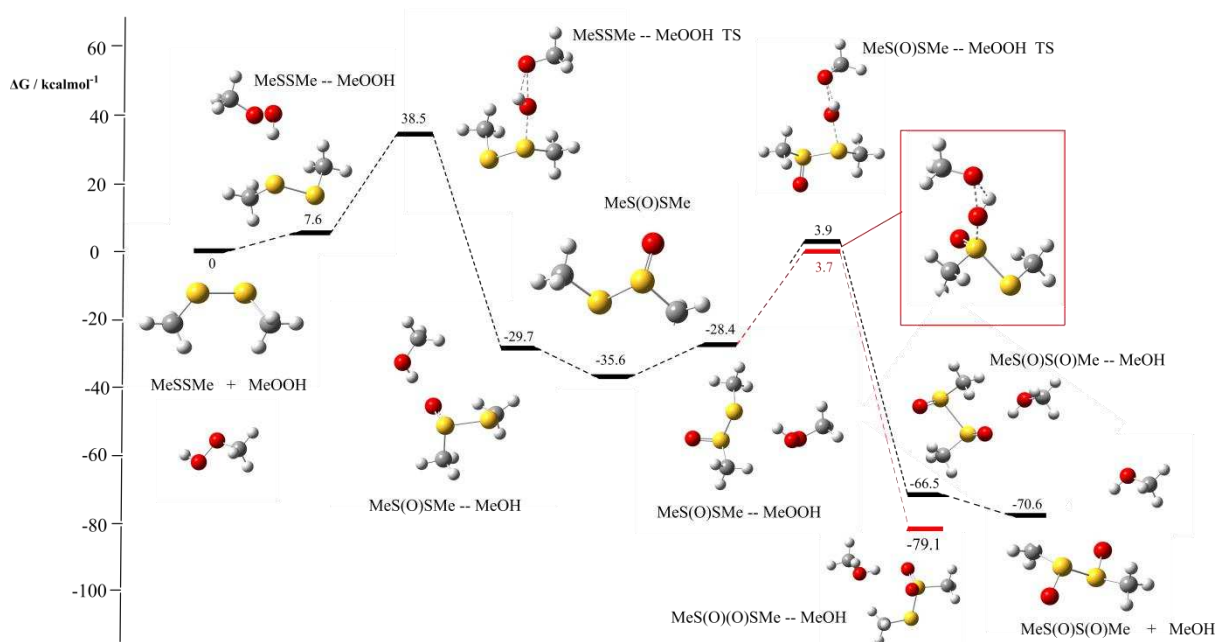
341

342 Disulfides, with the general formula  $\text{RSSR}$  can potentially undergo as many as four oxidations  
 343 with hydroperoxides. After the first oxidation, the second can occur at either the non-oxidized  
 344 or oxidized sulfur atom as summarized in **Scheme 2**, leading to a second oxidation species that  
 345 is either symmetric or asymmetric. However further oxidations will lead to the same end  
 346 product.

347

348 The free energy profile for the reaction of dimethyldisulfide and  $\text{MeOOH}$  up to and including  
 349 the second oxidation *via* the two different routes is shown in **Figure 12**. The initial oxidation  
 350 has an activation energy of  $38.5 \text{ kcal mol}^{-1}$ , which is comparable to the activation free energy  
 351 calculated for  $\text{RSH}$  oxidation in **Figure 8**. The activation free energies for the 2<sup>nd</sup> oxidation  
 352 are  $39.3$  and  $39.5 \text{ kcal mol}^{-1}$  for symmetric and asymmetric oxidation respectively. This

353 indicates that there is almost no kinetic preference as to which sulfur atom will be oxidized  
 354 after the initial oxidation  
 355



356  
 357 **Figure 13:** Gibbs free energy profile for the reaction of MeSSMe and MeOOH up to and  
 358 including the second oxidation.

359  
 360 Corresponding activation free energies for the reaction of CHP and MeSSMe are 38.2 kcal mol<sup>-1</sup>  
 361 and 39.2 kcal mol<sup>-1</sup> for the conversion of MeSSMe to MeS(O)SMe and MeS(O)SMe to  
 362 MeS(O)S(O)Me respectively.

363  
 364 Oxidation is not the only reaction that disulfides can undergo. In particular, disulfides contain  
 365 a diheteroatomic bond in much the same way as hydroperoxides and could potentially undergo  
 366 a fission reaction to form two thiyl radical species which are known to be very reactive.  
 367 Breaking of the disulfide bond will be easier if there is a significant weakening of the bond  
 368 during the autoxidation process, as indicated by a lengthening of the S-S bond and  
 369 consequentially change in the bond enthalpy.

370

371 The calculated bond enthalpies and corresponding S-S bond lengths for all of the potential  
372 species along the reaction coordinate are given in **Table 4**. The calculated S-S bond enthalpies  
373 for RSSR are 54 and 53 kcal mol<sup>-1</sup> for R=Me and <sup>n</sup>Bu respectively. These values are  
374 comparable to literature values for disulfide bonds that are generally around 50-60 kcal mol<sup>-1</sup>  
375 <sup>1,56</sup> **Table 4** shows that the first and second oxidations appreciably weaken the disulfide bond.  
376 Therefore fission of the S-S bond under autoxidation conditions should be considered in more  
377 detail.

378 **Table 4:** S-S bond lengths and enthalpies for a series of disulfide species.

Disulfide species	Bond enthalpy / kcal mol <sup>-1</sup>		Bond Length / Å	
	R = Me	R = <sup>n</sup> Bu	R = Me	R = <sup>n</sup> Bu
RSSR	54	53	2.068	2.092
RSOSR	32	32	2.167	2.235
RSOSOR	9	11	2.329	2.387
RSO <sub>2</sub> SOR	18	18	2.310	2.389
RSO <sub>2</sub> SO <sub>2</sub> R	25	24	2.285	2.343

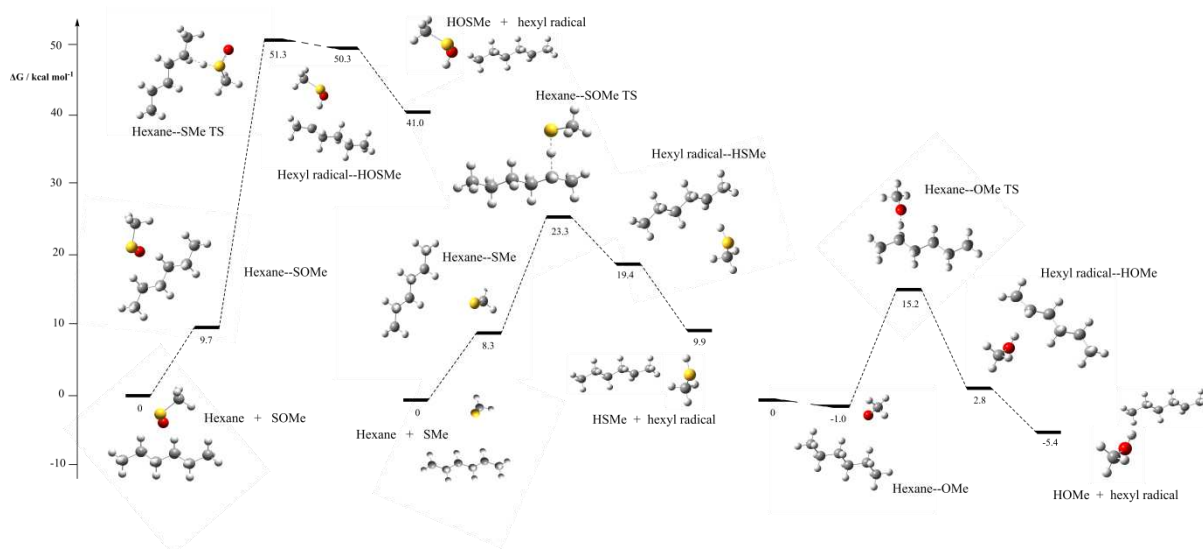
379

380 Our calculations show that the S-S bond significantly weakens upon successive oxidations.  
381 Even after a single oxidation, the activation free energy for the cleavage of the S-S bond  
382 becomes competitive with subsequent oxidations. Thus, the likely products from bond fission  
383 in these species are RSO● and RS●. Indeed, comparison with the activation free energy for  
384 RS(O)S(O)R formation, it is as likely to undergo bond fission than react with hydroperoxide.  
385 This is further substantiated by comparison of the frequency factors for both reactions (1.2E+22  
386 for bond fission and 1.8E+06 for the oxidation reaction). Whilst RSO<sub>2</sub>● can potentially form,  
387 the weakness of the S-S bond in RSOSOR makes this unlikely. We note that RSO● and RS●  
388 are relatable to the radical species formed during hydroperoxide fission, RO● and HO●, which  
389 are known to have critical roles in the autoxidation mechanism in fuels. Thus, it was

390 investigated whether any of the radicals that could potentially originate from disulfide fission  
391 could react with the bulk fuel in a similar way to peroxy radicals.

392

393 The free energy profile for the reaction of  $\text{MeSO}\bullet$  and  $\text{MeS}\bullet$  with bulk fuel is shown in **Figure**  
394 **13**. For comparison, an equivalent profile was calculated for the reaction of  $\text{MeO}\bullet$  and bulk  
395 fuel. In these reactions, hexane was used as a model for the hydrocarbons typically found in  
396 jet fuel to reduce the computational cost of the calculations. This approach can be justified as  
397 the reduction in chain length is not expected to have a significant effect on the reaction at the  
398 C2 carbon in the chain based upon previous studies.<sup>53</sup>

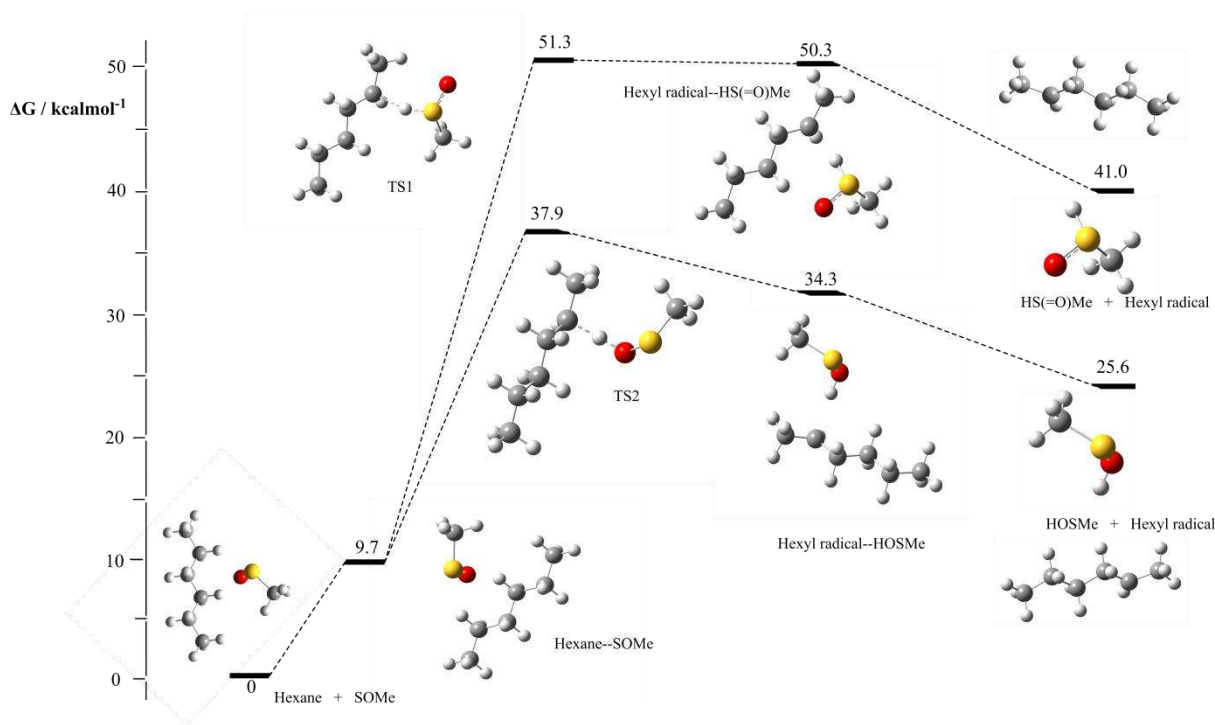


399

400 **Figure 13:** Gibbs free energy profile for the reaction of (left to right)  $\text{MeS(O)}\bullet$ ,  $\text{MeS}\bullet$  and  
401  $\text{MeO}\bullet$  with hexane.

402 The activation free energies for the reaction of  $\text{MeS}\bullet$ ,  $\text{MeS(O)}\bullet$  and  $\text{MeO}\bullet$  with bulk fuel are  
403 calculated to be 51.3, 23.3 and 15.2  $\text{kcal mol}^{-1}$ , respectively. Thus, the calculated activation  
404 free energy is appreciably larger for any of the sulfur species than for  $\text{MeO}\bullet$ . Moreover, the  
405 reactions involving sulfur radicals are significantly endothermic. This indicates that the sulfur  
406 radical is better stabilized than a carbon radical.

407 In the above it was assumed that hydrogen abstraction happens through sulfur, i.e. that the  
 408 radical character is localized there. However, a reaction could also happen through the oxygen  
 409 atom. A comparison of the two energy profiles is shown in **Figure 14**.



410

411 **Figure 14:** Gibbs free energy profile for the reaction of MeS(O)• and MeS•(O) with  
 412 hexane.

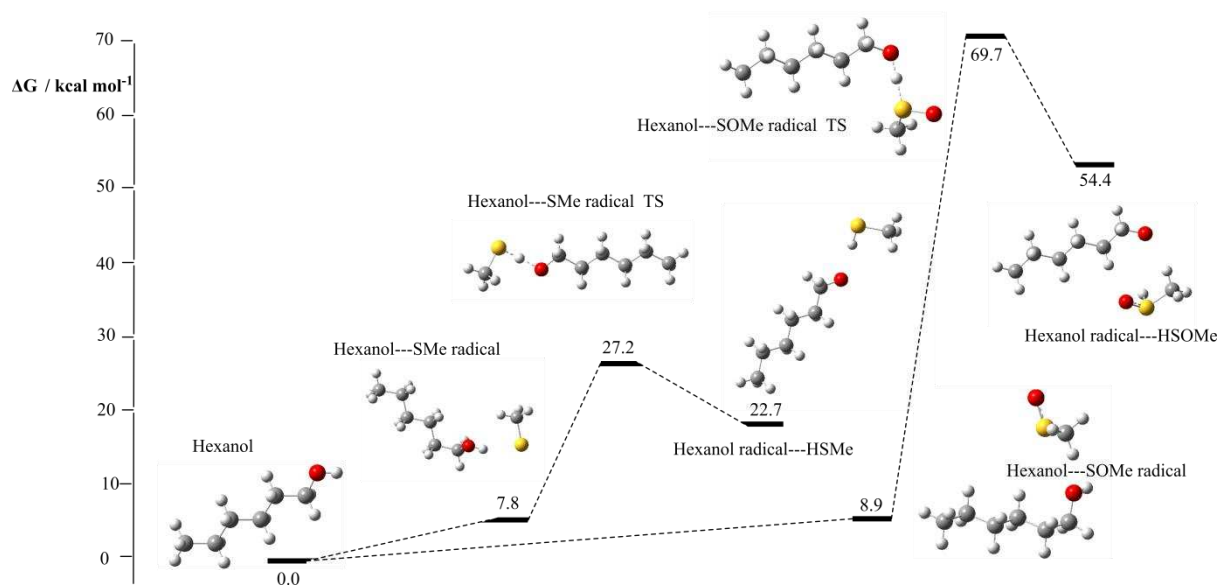
413 As can be seen, abstraction by oxygen is preferred over sulfur (activation free energies 37.9  
 414 and 51.3 kcal mol<sup>-1</sup>, respectively). However, even hydrogen abstraction by oxygen is still  
 415 endothermic. Overall, the data in **Figures 13** and **14** suggest that any radical sulfur species  
 416 formed from disulfide fission react less efficiently than radicals resulting from hydroperoxide  
 417 fission.

418

419 Our final consideration was whether the thiyl radicals, MeS• and MeS(O)•, could potentially  
 420 react with alcoholic species in the fuel. **Figure 15** shows the gibbs free energy profile for both  
 421 reactions. The reaction of hexanol and MeS• has a low kinetic barrier and will be



422 surmountable given typical autoxidation conditions. In contrast, the reaction of hexanol and  
423  $\text{MeS(O)}\bullet$  has a significantly higher Gibbs free activation energy, which is likely to be  
424 prohibitive. In both cases, the reaction is endothermic, which suggests that the radical is better  
425 stabilized when localized on the sulfur of the respective thiyl radical than the oxygen on  
426 hexanol.



427  
428 **Figure 15:** Gibbs free energy profile for the reaction of both  $\text{MeS(O)}\bullet$  and  $\text{MeS}\bullet(\text{O})$  with  
429 hexanol.

430

431

432

433

434

435

436

### 437 3.5 Mechanistic implications

438

439 The work undertaken herein has provided greater insight into the elementary reactions involved  
440 in the oxidation of sulfur species. Oxidation of sulfur species can lead to the formation of  
441 alcohols, sulfones, sulfoxides and sulfonic acids. Moreover, cleavage of disulfides can form  
442 thiyl radicals.

443

444 The presence of various sulfur species in jet fuel has the potential to retard the rate of  
445 autoxidation by reacting with hydroperoxides. The larger data set, consisting of a range of  
446 sulfur species reacting with different hydroperoxides, provides a more robust framework for  
447 the improvement of current chemical kinetic models. As mentioned previously, these models  
448 are of great importance for predicting the rate of autoxidation in jet fuels. In the widely used  
449 Kuprowicz mechanism there is a single reaction where sulfur is involved, which does not  
450 differentiate between the different classes of sulfur species in the fuel (equation 1).<sup>10</sup> This work  
451 would allow for the expansion of this single reaction into a series of reactions that not only  
452 differentiate between the classes of sulfur compounds but also the specific individual reactions  
453 that each one might undergo.

454

455 To more accurately represent the reactions that potentially could occur, we would propose  
456 supplementing equation 1 in the current kinetic mechanism with the reactions outlined in **Table**  
457 **5**, using the lumped data in **Table 6**. Reactions 1 to 4 describe the reactions of thiols and  
458 hydroperoxides. Reactions 5 and 6 describe the reactions of both thiophenes and sulfides with  
459 hydroperoxides. The reactions of disulfides and hydroperoxides are described by reactions 7-  
460 10.

461

**Table 5:** Proposed elementary steps to improve current chemical kinetic mechanisms

Elementary reaction step		Label
RSH + ROOH	$\longrightarrow$	RSO + ROH Reaction 1
RSO + ROOH	$\longrightarrow$	RSO <sub>2</sub> H + ROH Reaction 2
RSO <sub>2</sub> H + ROOH	$\longrightarrow$	RSO <sub>3</sub> H + ROH Reaction 3
RSR + ROOH	$\longrightarrow$	RSOR + ROH Reaction 4
RSOR + ROOH	$\longrightarrow$	RSO <sub>2</sub> R + ROH Reaction 5
RSSR + ROOH	$\longrightarrow$	RSOSR + ROH Reaction 6
RSOSR + ROOH	$\longrightarrow$	RSOSOR + ROH Reaction 7
RSOSOR + ROOH	$\longrightarrow$	RSO <sub>2</sub> SOR + ROH Reaction 8
RSO <sub>2</sub> SOR + ROOH	$\longrightarrow$	RSO <sub>3</sub> SO <sub>3</sub> R + ROH Reaction 9

463

464 The reactions, lumped activation energies and Arrhenius data for the elementary reactions  
 465 investigated herein are summarized in **Table 6**. With appropriate validation against  
 466 experimental data and testing to deduce the importance of each individual reaction, it is hoped  
 467 that this data will lead to a more accurate chemical kinetic model for fuel autoxidation.

468

469 **Table 6.** Lumped data for proposed steps to improve current chemical kinetic mechanisms.

470

(COH = Cumene hydroxide)

Sulfur species (Hydroperoxide)	Elementary reaction step	E <sub>a</sub> kcal mol <sup>-1</sup>	A mol <sup>-1</sup> s <sup>-1</sup>	Source
	SH + R'OOH $\longrightarrow$ Products <sub>SH</sub>	18	3E+09	Ref 10
<b>Thiols</b> (MeOOH)	RSH + MeOOH $\longrightarrow$ RSHO + MeOH	41.6	7.8E+05	This work
	RSO + MeOOH $\longrightarrow$ RSOH + MeOOH	19.2	4.0E+09	This work
	RSO <sub>2</sub> H + MeOOH $\longrightarrow$ RSO <sub>2</sub> H + MeOH	31.0	5.1E+09	This work
	RSO <sub>2</sub> H + MeOOH $\longrightarrow$ RSO <sub>3</sub> H + MeOH	38.9	1.9E+11	This work
<b>Thiols</b> (CHP)	RSH + CHP $\longrightarrow$ RSHO + COH	40.9	2.9E+05	This work
	RSO + CHP $\longrightarrow$ RSOH + CHP	23.9	1.9E+07	This work
	RSO <sub>2</sub> H + CHP $\longrightarrow$ RSO <sub>2</sub> H + COH	33.9	6.0E+08	This work
	RSO <sub>2</sub> H + CHP $\longrightarrow$ RSO <sub>3</sub> H + COH	41.1	1.9E+09	This work
<b>Thiols</b> ( <sup>t</sup> BuOOH)	RSH + <sup>t</sup> BuOOH $\longrightarrow$ RSHO + <sup>t</sup> BuOH	42.4	3.6E+05	This work
	RSO + <sup>t</sup> BuOOH $\longrightarrow$ RSOH + <sup>t</sup> BuOOH	20.2	3.5E+10	This work
	RSO <sub>2</sub> H + <sup>t</sup> BuOOH $\longrightarrow$ RSO <sub>2</sub> H + <sup>t</sup> BuOH	33.7	2.9E+10	This work
	RSO <sub>2</sub> H + <sup>t</sup> BuOOH $\longrightarrow$ RSO <sub>3</sub> H + <sup>t</sup> BuOH	42.3	3.0E+11	This work
<b>Sulfides</b> (MeOOH)	RSR + MeOOH $\longrightarrow$ RSOR + MeOH	36.9	9.6E+06	This work
	RSOR + MeOOH $\longrightarrow$ RSO <sub>2</sub> R + MeOH	37.3	2.3E+09	This work
<b>Sulfides</b>	RSR + CHP $\longrightarrow$ RSOR + COH	36.7	6.8E+05	This work

<b>(CHP)</b>	RSOR + CHP	—————>	RSO <sub>2</sub> R + COH	37.4	E+08	This work
<b>Sulfides</b>	RSR + 'BuOOH	—————>	RSOR + 'BuOH	37.9	6.8E+05	This work
<b>('BuOOH)</b>	RSOR + 'BuOOH	—————>	RSO <sub>2</sub> R + 'BuOH	39.6	2.2E+08	This work
<b>Disulfides</b>	RSSR + MeOOH	—————>	RSOSR + MeOH	39.9	6.5E+04	This work
<b>(MeOOH)</b>	RSOSR + MeOOH	—————>	RSOSOR + MeOH	39.3	1.3E+06	This work
	RSOSOR + MeOOH	—————>	RSO <sub>2</sub> SOR + MeOH	34.3	2.0E+09	This work
	RSO <sub>2</sub> SOR + MeOOH	—————>	RSO <sub>3</sub> SO <sub>3</sub> R + MeOH	38.3	1.1E+08	This work
<b>Disulfides</b>	RSSR + CHP	—————>	RSOSR + COH	41.9	1.3E+05	This work
<b>(CHP)</b>	RSOSR + CHP	—————>	RSOSOR + COH	41.6	3.8E+06	This work
	RSOSOR + CHP	—————>	RSO <sub>2</sub> SOR + COH	36.6	8.0E+06	This work
	RSO <sub>2</sub> SOR + CHP	—————>	RSO <sub>3</sub> SO <sub>3</sub> R + COH	38.9	1.4E+06	This work
<b>Disulfides</b>	RSSR + 'BuOOH	—————>	RSOSR + 'BuOH	39.8	5.8E+04	This work
<b>('BuOOH)</b>	RSOSR + 'BuOOH	—————>	RSOSOR + 'BuOH	40.6	5.4E+06	This work
	RSOSOR + 'BuOOH	—————>	RSO <sub>2</sub> SOR + 'BuOH	35.2	8.5E+06	This work
	RSO <sub>2</sub> SOR + 'BuOOH	—————>	RSO <sub>3</sub> SO <sub>3</sub> R + 'BuOH	38.9	2.2E+06	This work
<b>Thiophenes and</b>	RSR + MeOOH	—————>	RSOR + MeOH	45.4	8.3E+04	This work
<b>Benzothiophenes</b>	RSOR + MeOOH	—————>	RSO <sub>2</sub> R + MeOH	40.8	4.6E+09	This work
<b>(MeOOH)</b>						
<b>Thiophenes and</b>	RSR + CHP	—————>	RSOR + COH	47.6	1.3E+04	This work
<b>Benzothiophenes</b>	RSOR + CHP	—————>	RSO <sub>2</sub> R + COH	39.9	7.6E+08	This work
<b>(CHP)</b>						
<b>Thiophenes and</b>	RSR + 'BuOOH	—————>	RSOR + 'BuOH	46.3	1.2E+04	This work
<b>Benzothiophenes</b>	RSOR + 'BuOOH	—————>	RSO <sub>2</sub> R + 'BuOH	41.6	4.3E+08	This work
<b>('BuOOH)</b>						

471

## 472 4 Conclusions

473

474 In this work, we have reported on the reactions of a series of sulfur compounds with model  
475 hydroperoxides for those found in jet fuel. Thiols can react with up to four equivalents of  
476 peroxides *via* a sulfenic acid to form sulfonic acids and alcohols. In contrast, sulfides can only  
477 react with two equivalents of peroxides and form sulfones as opposed to sulfonic acids.

478

479 The reaction of disulfide species with hydroperoxides generally have a higher activation energy  
480 compared to thiols and sulfides. These sulfur species can potentially react with multiple  
481 equivalents of peroxides to form sulfones. Each successive oxidation acts to weaken the sulfur-  
482 sulfur bond, which facilitates the homolytic fission reaction to form thiyl radicals. Our results  
483 indicate that these radicals do not favourably react with bulk fuel components

484

485 Once appropriately validated, current chemical kinetic models for the autoxidation of jet fuel  
486 will be improved with the inclusion of the more detailed individual reactions investigated here.  
487 This flexibility will also allow tailoring of the kinetic scheme to account for specific species of  
488 sulfur present in specific fuels.

489

### 490 **Supporting Information**

491

492 Cartesian coordinates for DFT-optimized structures. Raw GC data resulting from the  
493 speciation analysis. Collated thermochemical data for all species investigated.

494

495

### 496 **Author information**

#### 497 **Corresponding Author**

498 Christopher Parks – Department of Mechanical Engineering, The University of Sheffield,  
499 Sheffield S3 7RD, U.K.; [orcid.org/0000-0001-8016-474X](https://orcid.org/0000-0001-8016-474X); Email: [c.m.parks@sheffield.ac.uk](mailto:c.m.parks@sheffield.ac.uk)

#### 500 **Authors**

501 Anthony J. H. M. Meijer - Department of Chemistry, The University of Sheffield, Sheffield,  
502 S3 7HF.; [orcid.org/0000-0003-4803-3488](https://orcid.org/0000-0003-4803-3488)

503 Simon. Blakey - Department of Mechanical Engineering, The University of Birmingham,  
504 Birmingham B15 2TT, U.K.

505 Ehsan Alborzi – Department of Mechanical Engineering, The University of Sheffield,  
506 Sheffield S3 7RD, U.K.; [orcid.org/0000-0002-2585-0824](https://orcid.org/0000-0002-2585-0824)

507 Mohamed Pourkashanian – Department of Mechanical Engineering, The University of  
508 Sheffield, Sheffield S3 7RD, U.K.

509

## 510 **Acknowledgments**

511

512 The research presented in this paper has been performed in the framework of the JETSCREEN  
513 project (JETfuel SCREENING and optimization) and has received funding from the European  
514 Union Horizon 2020 Programme under grant agreement n° 723525. The authors declare no  
515 competing financial interest.

516

517

518

## 519 **References**

520

- 521 1. Balster, L. M.; Zabarnick, S.; Striebich, R. C.; Shafer, L. M.; West, Z. J., Analysis of Polar  
522 Species in Jet Fuel and Determination of Their Role in Autoxidative Deposit Formation. *Energy &*  
523 *Fuels* **2006**, *20*, 2564–2571.
- 524 2. Taylor, W. F., Deposit Formation from Deoxygenated Hydrocarbons. II. Effect of Trace Sulfur  
525 Compounds. *Product R&D* **1976**, *15* (1), 64-68.
- 526 3. Zabarnick, S.; Mick, M. S., Inhibition of Jet Fuel Oxidation by Addition of Hydroperoxide-  
527 Decomposing Species. *Ind. Eng. Chem. Res.* **1999**, *38*, 3557–3563.
- 528 4. Ervin, J. S.; Williams, T. F., Dissolved Oxygen Concentration and Jet Fuel Deposition. *Ind. Eng.*  
529 *Chem. Res.* **1996**, *35*, 899–904.
- 530 5. Grinstead, B.; Zabarnick, S., Studies of Jet Fuel Thermal Stability, Oxidation, and Additives  
531 Using an Isothermal Oxidation Apparatus Equipped with an Oxygen Sensor. *Energy & Fuels* **1999**, *13*,  
532 756–760.
- 533 6. Jones, E. G.; Balster, L. M., Impact of Additives on the Autoxidation of a Thermally Stable  
534 Aviation Fuel. *Energy & Fuels* **1997**, *11*, 610-614.

- 535 7. Striebich, R. C.; Contreras, J.; Balster, L. M.; West, Z.; Shafer, L. M.; Zabarnick, S.,  
536 Identification of Polar Species in Aviation Fuels using Multidimensional Gas Chromatography-Time of  
537 Flight Mass Spectrometry. *Energy & Fuels* **2009**, *23*, 5474–5482.
- 538 8. Taylor, W. F.; Frankenfeld, J. W., Deposit Formation from Deoxygenated Hydrocarbons. 3.  
539 Effects of Trace Nitrogen and Oxygen Compounds. *Ind. Eng. Chem. Prod. Res. Dev.* **1978**, *17*, 86–90.
- 540 9. Zabarnick, S.; West, Z. J.; Shafer, L. M.; Mueller, S. S.; Striebich, R. C.; Wrzesinski, P. J.,  
541 Studies of the Role of Heteroatomic Species in Jet Fuel Thermal Stability: Model Fuel Mixtures and  
542 Real Fuels. *Energy & Fuels* **2019**, *33* (9), 8557-8565.
- 543 10. Kuprowicz, N. J.; Zabarnick, S.; West, Z. J.; Ervin, J. S., Use of Measured Species Class  
544 Concentrations with Chemical Kinetic Modeling for the Prediction of Autoxidation and Deposition of  
545 Jet Fuels. *Energy & Fuels* **2007**, *21* (2), 530-544.
- 546 11. Pickard, J. M.; Jones, E. G., Catalysis of Jet-A Fuel Autoxidation by Fe<sub>2</sub>O<sub>3</sub>. *Energy & Fuels*  
547 **1997**, *11*, 1232–1236.
- 548 12. West, Z. J.; Zabarnick, S.; Striebich, R. C., Determination of Hydroperoxides in Jet Fuel via  
549 Reaction with Triphenylphosphine. *Industrial & Engineering Chemistry Research* **2005**, *44* (10), 3377-  
550 3383.
- 551 13. Zabarnick, S., Chemical kinetic modeling of jet fuel autoxidation and antioxidant chemistry.  
552 *Industrial & Engineering Chemistry Research* **1993**, *32* (6), 1012-1017.
- 553 14. Aksoy, P.; Gül, Ö.; Cetiner, R.; Fonseca, D. A.; Sobkowiak, M.; Falcone-Miller, S.; Miller, B.  
554 G.; Beaver, B., Insight into the Mechanisms of Middle Distillate Fuel Oxidative Degradation. Part 2:  
555 On the Relationship between Jet Fuel Thermal Oxidative Deposit, Soluble Macromolecular  
556 Oxidatively Reactive Species, and Smoke Point. *Energy & Fuels* **2009**, *23* (4), 2047-2051.
- 557 15. Ben Amara, A.; Kaoubi, S.; Starck, L., Toward an optimal formulation of alternative jet fuels:  
558 Enhanced oxidation and thermal stability by the addition of cyclic molecules. *Fuel* **2016**, *173*, 98-105.
- 559 16. Chatelain, K.; Nicolle, A.; Ben Amara, A.; Catoire, L.; Starck, L., Wide Range Experimental  
560 and Kinetic Modeling Study of Chain Length Impact on n-Alkanes Autoxidation. *Energy & Fuels* **2016**,  
561 *30* (2), 1294-1303.
- 562 17. Galano, A.; Alvarez-Idaboy, J. R., Kinetics of radical-molecule reactions in aqueous solution: A  
563 benchmark study of the performance of density functional methods. *Journal of Computational*  
564 *Chemistry* **2014**, *35* (28), 2019-2026.
- 565 18. Gül, Ö.; Cetiner, R.; Griffith, J. M.; Wang, B.; Sobkowiak, M.; Fonseca, D. A.; Aksoy, P.;  
566 Miller, B. G.; Beaver, B., Insight into the Mechanisms of Middle Distillate Fuel Oxidative Degradation.  
567 Part 3: Hydrocarbon Stabilizers to Improve Jet Fuel Thermal Oxidative Stability. *Energy & Fuels* **2009**,  
568 *23* (4), 2052-2055.

- 569 19. Jalan, A.; Alecu, I. M.; Meana-Pañeda, R.; Aguilera-Iparraguirre, J.; Yang, K. R.; Merchant,  
570 S. S.; Truhlar, D. G.; Green, W. H., New Pathways for Formation of Acids and Carbonyl Products in  
571 Low-Temperature Oxidation: The Korcek Decomposition of  $\gamma$ -Ketohydroperoxides. *Journal of the*  
572 *American Chemical Society* **2013**, *135* (30), 11100-11114.
- 573 20. Mangiatordi, G. F.; Brémond, E.; Adamo, C., DFT and Proton Transfer Reactions: A  
574 Benchmark Study on Structure and Kinetics. *Journal of Chemical Theory and Computation* **2012**, *8*  
575 (9), 3082-3088.
- 576 21. Park, S. H.; Kwon, C. H.; Kim, J.; Han, J. S.; Jeong, B. H.; Han, H.; Kim, S. H., Mechanistic  
577 Insights into Oxidative Decomposition of exo-Tetrahydrodicyclopentadiene. *The Journal of Physical*  
578 *Chemistry C* **2013**, *117* (31), 15933-15939.
- 579 22. Lobodin, V. V.; Robbins, W. K.; Lu, J.; Rodgers, R. P., Separation and Characterization of  
580 Reactive and Non-Reactive Sulfur in Petroleum and Its Fractions. *Energy & Fuels* **2015**, *29* (10), 6177-  
581 6186.
- 582 23. Link, D. D.; Baltrus, J. P.; Rothenberger, K. S.; Zandhuis, P.; Minus, D. K.; Striebich, R. C.,  
583 Class- and Structure-Specific Separation, Analysis, and Identification Techniques for the  
584 Characterization of the Sulfur Components of JP-8 Aviation Fuel. *Energy & Fuels* **2003**, *17* (5), 1292-  
585 1302.
- 586 24. Stumpf, Á.; Tolvaj, K.; Juhász, M., Detailed analysis of sulfur compounds in gasoline range  
587 petroleum products with high-resolution gas chromatography–atomic emission detection using  
588 group-selective chemical treatment. *Journal of Chromatography A* **1998**, *819* (1), 67-74.
- 589 25. Batts, B. D.; Fathoni, A. Z., A literature review on fuel stability studies with particular  
590 emphasis on diesel oil. *Energy & Fuels* **1991**, *5* (1), 2-21.
- 591 26. de Souza, W. F.; Guimarães, I. R.; Guerreiro, M. C.; Oliveira, L. C. A., Catalytic oxidation of  
592 sulfur and nitrogen compounds from diesel fuel. *Applied Catalysis A: General* **2009**, *360* (2), 205-209.
- 593 27. Fathoni, A. Z.; Batts, B. D., A literature review of fuel stability studies with a particular  
594 emphasis on shale oil. *Energy & Fuels* **1992**, *6* (6), 681-693.
- 595 28. Kendall, D. R.; Clark, R. H.; Wolveridge, P. E., Fuels for Jet Engines: The Importance of  
596 Thermal Stability. *Aircraft Engineering and Aerospace Technology* **1987**, *59* (12), 2-7.
- 597 29. Mushrush, G. W.; Hazlett, R. N.; Pellenbarg, R. E.; Hardy, D. R., Role of sulfur compounds in  
598 fuel instability: a model study of the formation of sulfonic acids from hexyl sulfide and hexyl  
599 disulfide. *Energy & Fuels* **1991**, *5* (2), 258-262.
- 600 30. Zabarnick, S.; Phelps, D. K., Density Functional Theory Calculations of the Energetics and  
601 Kinetics of Jet Fuel Autoxidation Reactions. *Energy & Fuels* **2006**, *20* (2), 488-497.



- 602 31. Hiley, R. W.; Pedley, J. F., Storage stability of petroleum-derived diesel fuel: 2. The effect of  
603 sulphonic acids on the stability of diesel fuels and a diesel fuel extract. *Fuel* **1988**, *67* (4), 469-473.
- 604 32. Offenhauer, R. D.; Brennan, J. A.; Miller, R. C., Sediment Formation in Catalytically Cracked  
605 Distillate Fuel Oils. *Industrial & Engineering Chemistry* **1957**, *49* (8), 1265-1266.
- 606 33. Denison, G. H., Oxidation of Lubricating Oils. *Industrial & Engineering Chemistry* **1944**, *36* (5),  
607 477-482.
- 608 34. Thompson, R. B.; Druge, L. W.; Chenicek, J. A., Stability of Fuel Oils in Storage: Effect of  
609 Sulfur Compounds. *Industrial & Engineering Chemistry* **1949**, *41* (12), 2715-2721.
- 610 35. Daniel, S. R.; Heneman, F. C., Deposit formation in liquid fuels: 4. Effect of selected organo-  
611 sulphur compounds on the stability of Jet A fuel. *Fuel* **1983**, *62* (11), 1265-1268.
- 612 36. Rawson, P. M.; Webster, R. L.; Evans, D.; Abanteriba, S., Contribution of sulfur compounds  
613 to deposit formation in jet fuels at 140 °C using a quartz crystal microbalance technique. *Fuel* **2018**,  
614 *231*, 1-7.
- 615 37. Bach, R. D.; Dmitrenko, O., Electronic Requirements for Oxygen Atom Transfer from Alkyl  
616 Hydroperoxides. Model Studies on Multisubstrate Flavin-Containing Monooxygenases. *The Journal*  
617 *of Physical Chemistry B* **2003**, *107* (46), 12851-12861.
- 618 38. Beens, J.; Tijssen, R., The characterization and quantitation of sulfur-containing compounds  
619 in (heavy) middle distillates by LC-GC-FID-SCD. *Journal of High Resolution Chromatography* **1997**, *20*  
620 (3), 131-137.
- 621 39. Ruiz-Guerrero, R.; Vendeuvre, C.; Thiébaud, D.; Bertoncini, F.; Espinat, D., Comparison of  
622 Comprehensive Two-Dimensional Gas Chromatography Coupled with Sulfur-Chemiluminescence  
623 Detector to Standard Methods for Speciation of Sulfur-Containing Compounds in Middle Distillates.  
624 *Journal of Chromatographic Science* **2006**, *44* (9), 566-573.
- 625 40. Wang, F. C.-Y.; Robbins, W. K.; Di Sanzo, F. P.; McElroy, F. C., Speciation of Sulfur-Containing  
626 Compounds in Diesel by Comprehensive Two-Dimensional Gas Chromatography. *Journal of*  
627 *Chromatographic Science* **2003**, *41* (10), 519-523.
- 628 41. M. J. Frisch; G. W. Trucks; H. B. Schlegel; G. E. Scuseria; M. A. Robb; J. R. Cheeseman; G.  
629 Scalmani; V. Barone; B. Mennucci; G. A. Petersson; H. Nakatsuji; M. Caricato; X. Li; H. P.  
630 Hratchian; A. F. Izmaylov; J. Bloino; G. Zheng; J. L. Sonnenberg; M. Hada; M. Ehara; K. Toyota; R.  
631 Fukuda; J. Hasegawa; M. Ishida; T. Nakajima; Y. Honda; O. Kitao; H. Nakai; T. Vreven; J. A.  
632 Montgomery, J.; J. E. Peralta; F. Ogliaro; M. Bearpark; J. J. Heyd; E. Brothers; K. N. Kudin; V. N.  
633 Staroverov; T. Keith; R. Kobayashi; J. Normand; K. Raghavachari; A. Rendell; J. C. Burant; S. S.  
634 Iyengar; J. Tomasi; M. Cossi; N. Rega; J. M. Millam; M. Klene; J. E. Knox; J. B. Cross; V. Bakken; C.  
635 Adamo; J. Jaramillo; R. Gomperts; R. E. Stratmann; O. Yazyev; A. J. Austin; R. Cammi; C. Pomelli, J.

636 W. O.; R. L. Martin; K. Morokuma; V. G. Zakrzewski; G. A. Voth; P. Salvador; J. J. Dannenberg; S.  
637 Dapprich; A. D. Daniels; O. Farkas; J. B. Foresman; J. V. Ortiz; J. Cioslowski; Fox, D. J. *Gaussian 09*,  
638 2016.

639 42. Clint Whaley, R.; Petitet, A.; Dongarra, J. J., Automated empirical optimizations of software  
640 and the ATLAS project. *Parallel Computing* **2001**, *27* (1), 3-35.

641 43. Whaley, R. C.; Petitet, A., Minimizing development and maintenance costs in supporting  
642 persistently optimized BLAS. *Software: Practice and Experience* **2005**, *35* (2), 101-121.

643 44. Becke, A. D., Density-functional exchange-energy approximation with correct asymptotic  
644 behavior. *Physical Review A* **1988**, *38* (6), 3098-3100.

645 45. Lee, C.; Yang, W.; Parr, R. G., Development of the Colle-Salvetti correlation-energy formula  
646 into a functional of the electron density. *Physical Review B* **1988**, *37* (2), 785-789.

647 46. Perdew, J. P.; Chevary, J. A.; Vosko, S. H.; Jackson, K. A.; Pederson, M. R.; Singh, D. J.;  
648 Fiolhais, C., Atoms, molecules, solids, and surfaces: Applications of the generalized gradient  
649 approximation for exchange and correlation. *Physical Review B* **1992**, *46* (11), 6671-6687.

650 47. Dunning Jr., T. H., Gaussian basis sets for use in correlated molecular calculations. I. The  
651 atoms boron through neon and hydrogen. *The Journal of Chemical Physics* **1989**, *90* (2), 1007-1023.

652 48. Cossi, M.; Barone, V., Analytical second derivatives of the free energy in solution by  
653 polarizable continuum models. *The Journal of Chemical Physics* **1998**, *109* (15), 6246-6254.

654 49. Scalmani, G.; Frisch, M. J., Continuous surface charge polarizable continuum models of  
655 solvation. I. General formalism. *The Journal of Chemical Physics* **2010**, *132* (11), 114110.

656 50. Cancès, E.; Mennucci, B.; Tomasi, J., A new integral equation formalism for the polarizable  
657 continuum model: Theoretical background and applications to isotropic and anisotropic dielectrics.  
658 *The Journal of Chemical Physics* **1997**, *107* (8), 3032-3041.

659 51. Funes-Ardoiz, I.; Paton, R. S. GoodVibes: Version 2.0.3. Zenodo 2018.

660 52. Werner, H.-J.; Knowles, P. J.; Knizia, G.; Manby, F. R.; Schütz, M., Molpro: a general-  
661 purpose quantum chemistry program package. *WIREs Computational Molecular Science* **2012**, *2* (2),  
662 242-253.

663 53. Parks, C. M.; Alborzi, E.; Blakey, S. G.; Meijer, A. J. H. M.; Pourkashanian, M., Density  
664 Functional Theory Calculations on Copper-Mediated Peroxide Decomposition Reactions: Implications  
665 for Jet Fuel Autoxidation. *Energy & Fuels* **2020**, *34* (6), 7439-7447.

666 54. Alborzi, E.; Parks, C. M.; Gadsby, P.; Sheikhsari, A.; Blakey, S. G.; Pourkashanian, M.,  
667 Effect of Reactive Sulfur Removal by Activated Carbon on Aviation Fuel Thermal Stability. *Energy &*  
668 *Fuels* **2020**, *34* (6), 6780-6790.

- 669 55. Lu, Y.; Dong, Z.; Wang, P.; Zhou, H.-B., Thiophene Oxidation and Reduction Chemistry. In  
670 *Thiophenes*, Joule, J. A., Ed. Springer International Publishing: Cham, 2015; pp 227-293.
- 671 56. Denk, M. K., The Variable Strength of the Sulfur–Sulfur Bond: 78 to 41 kcal – G3, CBS-Q, and  
672 DFT Bond Energies of Sulfur (S8) and Disulfanes XSSX (X = H, F, Cl, CH3, CN, NH2, OH, SH). *European*  
673 *Journal of Inorganic Chemistry* **2009**, 2009 (10), 1358-1368.

674